PASSIVE MICROWAVE REMOTE SENSING OF SOIL MOISTURE

Eni G. Njoku[1] and Dara Entekhabi[2]

[1] Jet Propulsion Laboratory
California Institute of Technology
Pasadena, CA 91109

[2] Department of Civil and Environmental Engineering
Massachusetts Institute of Technology
Cambridge, Massachusetts 02139

Submitted to:
Journal of Hydrology

August, 1994

[1] Address for correspondence: Dr. Eni G. Njoku, M/S 300-233, Jet Propulsion Laboratory, 4800 Oak Grove Drive, Pasadena, CA 91109.

Abstract

Microwave remote sensing provides a unique capability for direct observation of soil moisture. Remote measurements from space afford the possibility of obtaining frequent, global sampling of soil moisture over a large fraction of the Earth's land surface. Microwave measurements have the benefit of being largely unaffected by solar illumination and cloud cover, but accurate soil moisture estimates are limited to regions that have either bare soil or low to moderate amounts of vegetation cover. A particular advantage of passive microwave sensors is that in the absence of significant vegetation cover soil moisture is the dominant effect on the received signal. The spatial resolutions of passive microwave soil moisture sensors currently conceived for space operation are in the range 10-20 km, The most useful frequency range for soil moisture sensing is 1-5 GHz. A particular system design requires an optimum choice of frequencies, polarizations, and scanning configurations based on trade-offs between considerations of high vegetation penetration capability, freedom from electromagnetic interference, manageable antenna size and complexity, and the requirement for sufficient information channels to correct for perturbing geophysical effects. This paper outlines the basic principles of the passive microwave technique for soil moisture sensing, and reviews briefly the status of current retrieval methods, Particularly promising are methods for optimally assimilating passive microwave data into hydrologic models.

1.0 INTRODUCTION

The emission of thermal microwave radiation from soil is strongly dependent on the soil moisture content. The difference between the dielectric constant of water (-80 at frequencies below 5 GHz) and that of dry soil (-3.5) is very large; as a result the emissivity of soils varies over a wide range from approximately 0.6 for wet (saturated) soils to greater than 0.9 for dry soils. For a soil at a temperature of, say, 300 K this range in emissivity corresponds to a soil brightness temperature variation of 90 K (covering a range of wetness from -40% to -5% moisture by volume depending on the soil type). This variation in brightness may be compared to the measurement sensitivity of a microwave radiometer which is typically better than 1 K. The large available signal to noise ratio is the basis of the passive microwave technique for soil moisture remote sensing. For a bare soil, moisture estimation accuracies of 1-2% by volume are feasible in principle.

Such accuracies are difficult to achieve in practice. The soil brightness temperature is also affected by vegetation and soil surface roughness and, to a lesser degree, by soil and vegetation temperature and soil texture. These perturbing factors introduce varying amounts of uncertainty into the relationships between brightness temperature and soil moisture, thereby limiting the accuracy with which soil moisture can be estimated. However, towards the longer wavelength region of the microwave spectrum (wavelength λ > -10 cm) the effects. of vegetation and roughness become much reduced. At these wavelengths, in areas of low to moderate vegetation, the soil moisture content has a dominant effect on the brightness temperature. Furthermore, vegetation and roughness have different spectral and polarization effects than soil moisture on the soil brightness, making it is possible to correct for these perturbations by making multifrequency, multipolarization measurements. Information from other sources such as visible, infrared and active microwave remote sensing measurements, and ancillary surface data such as digitized maps of land surface cover, soil types, and topography, can also be helpful in improving the soil moisture estimates.

The low-frequency microwave range of 1-3 GHz (30-10 cm wavelength) is considered optimum for soil moisture sensing due to the reduced atmospheric attenuation and greater vegetation penetration at these longer wavelengths, Most studies have focused on a frequency of 1.4 GHz since this is in a protected radio astronomy band where radio frequency interference (RFI) is at a minimum. At frequencies of 1.4 GHz and below the large antenna size required to obtain reasonable spatial resolution on the ground becomes an

increasingly difficult technological problem. RFI, Faraday rotation and galactic noise also become increasingly significant error sources at frequencies below 1.4 GHz. During the past two decades, experimental measurements carried out using ground-based and aircraft radiometers, and some limited satellite observations, have demonstrated the basic principles and feasibility of soil moisture estimation. Large-scale operational demonstrations have been difficult, however. There has been no low-frequency radiometer system operating continuously in space with which to obtain large-area repetitive measurements "over annual or even seasonal time scales. There is also the difficulty of obtaining representative in situ measurements of soil moisture over large areas for validating the remote sensing observations. Efforts are underway to develop a low-frequency spaceborne passive microwave soil moisture sensor for operational demonstration, One such concept is the Electronically Scanned Thinned Array Radiometer(ESTAR) (Swift, 1993).

This paper reviews briefly the theoretical and experimental background to remote sensing of soil moisture using passive microwaves, highlighting some of the more important issues of sensitivity and retrievability. A discussion of soil moisture retrieval approaches and recent experimental results is also provided.

2.0 MICROWAVE EMISSION FROM SOILS

Figure 1 is a schematic view of a radiometer viewing the Earth's surface from a remote platform. The surface area viewed by the radiometer antenna may be considered to include bare soil, vegetation, or a heterogeneous mixture of soil and vegetation types. We begin by discussing microwave emission from bare, smooth, homogeneous soils, with uniform subsurface moisture and temperature, in order to illustrate the main concepts of thermal radiation and emissivity, and to discuss the effects of soil moisture, soil texture, and surface temperature on the emitted radiation. Subsequently we discuss the effects of nonuniform soil profiles, surface roughness, and vegetation on the emitted radiation. The effects of propagation through the atmosphere will not be dealt with since at the lower microwave frequencies of interest in soil moisture sensing atmospheric effects are small and may be safely neglected in most cases. Similarly, volume scattering in the soil is negligible at these wavelengths and will not be considered here.

Surface imaging microwave radiometers are normally designed to measure thermally emitted microwave radiation in two orthogonal polarizations from a direction

defined by the antenna pattern of the receiving antenna. The receiving polarizations of the antenna can be straightforwardly related to the vertical and horizontal polarizations of radiation emitted from the Earth's surface (defined relative to the normal to the surface and the viewing direction of the antenna (ref)).

2.1 *Thermal Radiation and Surface Emissivity*

Thermal radiation emitted by the Earth's surface can be described by Planck's blackbody radiation law. At microwave wavelengths, and for temperatures typical of the Earth's surface, the Rayleigh-Jeans approximation ($h\nu << kT$) to Planck's law holds, and the specific intensity of blackbody radiation at temperature T (Kelvins) can be written:

$$I_0 = kT/\lambda^2 \tag{1}$$

where, ν is frequency (Hz), λ is wavelength (m), k is Boltzmann's constant, and I_0 has units of Watts/m^2/Hz/steradian. Since in this approximation the intensity is directly proportional to temperature, it is convenient to define the "brightness temperature" of general (nonblackbody) thermal radiation of intensity I by the expression: $T_b = \frac{I \lambda^2}{k}$. The relationship of the brightness temperature of a thermally radiating body to its true temperature T is then given by the simple expression:

$$T_b = eT \tag{2}$$

where e is the emissivity of the body and T_b is expressed in Kelvins (for a blackbody e = 1). This expression can be used to represent the brightness temperature of the Earth's surface at temperature T and emissivity e, at any given location, if the subsurface temperature profile is uniform (isothermal). Kirchoffs reciprocity theorem relates the emissivity to the reflectivity, r, of the surface:

$$e = 1 - r \tag{3}$$

The surface reflectivity may be computed from knowledge of the dielectric constant of the medium and the surface boundary condition. For a smooth surface, and uniform dielectric constant, the expressions for reflectivity are:

$$r_v = \left| \frac{\varepsilon_r \cos\theta - \sqrt{\varepsilon_r - \sin^2\theta}}{\varepsilon_r \cos\theta + \sqrt{\varepsilon_r - \sin^2\theta}} \right|^2$$

$$r_h = \left| \frac{\cos\theta - \sqrt{\varepsilon_r - \sin^2\theta}}{\cos\theta + \sqrt{\varepsilon_r - \sin^2\theta}} \right| \qquad (4)$$

where θ is the incidence angle (measured from the surface normal) and ε_r is the complex dielectric constant (relative permittivity) of the medium. The reflectivities, and hence the emissivities and brightness temperatures, thus depend on the dielectric constant, the incidence (i.e. viewing) angle, and the polarization of the radiation (vertical or horizontal).

2.2 Soil *Dielectric Properties*

The dielectric properties of wet soils have been studied in detail by several investigators (e.g. Wang and Schmugge, 1980; Dobson et al., 1985). The high dielectric constant of water significantly increases both the real and imaginary parts of the dielectric constant of the soil as the volume fraction of water in the soil increases. Figure 2 shows the relationship between dielectric constant and volumetric soil moisture content for a variety of soil types at a frequency of 1.4 GHz. The dependence on soil type (or "texture") is due to differences in the percentage of water bound to the particle surfaces in the different soils. Bound water is less freely able to exhibit molecular rotation at microwave frequencies and hence has a smaller dielectric effect than the free water in the pore spaces. This is most evident in clay soils which have greater particle surface areas and greater affinities for binding water molecules, and hence hold greater percentages of bound water. The dependence of dielectric constant on soil texture introduces some uncertainty into estimates of soil moisture if the soil textural composition is unknown.

The frequency dependence of soil dielectric constant is illustrated for a sandy soil in Figure 3. The shapes of the curves for the real and imaginary parts are determined primarily by the frequency dependence of the dielectric constant of water. At frequencies below 3-5 GHz there is little variability in the real part of the dielectric constant; hence there is little frequency dependence of the soil emissivity in this range (the emissivity is" determined primarily by the large real part of the dielectric constant), The imaginary part of the dielectric constant, does, however, exhibit a frequency dependence, and this leads to frequency-dependent attenuation of radiation through the medium. This can be quantified

by a parameter known as the "penetration depth", defined as the distance in the medium over which the intensity of the radiation decreases (due to attenuation) by a factor of I/e (i.e. by -63%). From the viewpoint of radiation emitted from a surface, the penetration depth is equivalent to the depth from above which 63% of the radiation emitted by the surface originates. The penetration depth can be expressed as:

$$\delta = \frac{\lambda}{4\pi n''} \tag{5}$$

where, n" is the imaginary part of the refractive index, n, of the medium, which is related to the dielectric constant by $n = \sqrt{\varepsilon_r}$. Figure 4 shows the dependence of penetration depth on wavelength and moisture content for a sandy soil (using the dielectric constant curves of Figure 3). At 1.5 GHz the penetration depth varies from approximately 10 cm to 1 m for soil conditions ranging from saturated to dry, while at 30 GHz the penetration depth varies from less than 1 mm to a little over 1 cm for similar conditions. The penetration depth is important because it is an indication of the depth below the surface within which variations in moisture and temperature significantly affect the emitted radiation. Longer wavelengths with greater penetration depths sense moisture and temperature changes deeper in the soil than shorter wavelengths.

The dielectric properties of wet soils are only weakly dependent on temperature, and for the range of soil temperatures encountered in nature the temperature dependence may be ignored. However, frozen soils have much lower dielectric constants than unfrozen soils since the contained water is no longer in the liquid phase (Hoekstra and Delaney, 1974). This feature has led to studies of microwave radiometry for detecting areas of permafrost and freeze-thaw boundaries in soils.

Figures 5 and 6 show the computed dependence of emissivity on moisture content and viewing angle, respectively, for bare, smooth soil. In Figure 5, data from radiometric observations are also shown, indicating the good agreement between observed and computed emissivities typically obtained in such experiments.

2.3 *Nonuniform Moisture and Temperature*

The temperatures and moisture contents of soils exhibit natural variability as functions of depth. It is not strictly correct therefore to represent soil brightness

temperature and emissivity by expressions such as Equations (2) and (4) which assume uniform temperature and dielectric constant, respectively. This is especially the case at longer wavelengths which may respond to moisture and temperature conditions over depths of several centimeters below the surface, over which the profiles may vary significantly.

When the subsurface moisture profile varies slowly with respect to the wavelength in the medium the incoherent radiative transfer approximation can be used to express the surface brightness temperature as:

$$T_b = e\left\{\int_{-\infty}^{0} T(z)\, et(z) \exp\left[-\int_{z}^{0} \alpha(z')\, dz'\right] dz\right\} \qquad (6)$$

The attenuation coefficient in the soil, et(z), depends on the dielectric constant, and, for nadir viewing, can be expressed simply as $\alpha(z) = 4\pi n$ "(z) / λ. Equation (6) is similar to Equation (2) except that it more correctly expresses&e brightness temperature in terms of an "effective temperature" T_e, given by the integral expression in curly brackets, instead of the surface temperature, T. The effective temperature is a weighted mean of the vertical temperature profile T(z) and may differ substantially from the surface temperature for dry soils. Figure 7 shows scatterplots of computed effective temperature versus surface temperature for a range of soil moisture and temperature profiles (Choudhury et al., 1982). The profiles are typical of semi-arid regions which exhibit fairly large extremes in diurnal surface temperature. Profiles typical of more humid environments exhibit less surface temperature variability. Variability in the soil effective temperature is a potential error source in estimating soil moisture from measurements of brightness temperature. The variability decreases at longer wavelengths due to the greater penetration depths.

In cases where the subsurface dielectric properties vary rapidly with respect to wavelength in the medium Equation (7) becomes inaccurate and the brightness temperature must be modeled instead using a coherent electromagnetic wave approach (see Tsang et al., 1975 or Njoku and Kong, 1977 for a full description of this approach). A coherent wave treatment is necessary to interpret the effects of sharp discontinuities in the soil moisture profiles, such as may occur between a dry surface crust and wetter soil below *or* where there is saturated soil (water table) close to the surface.

With a nonuniform moisture profile the penetration depth can no longer be defined simply as in Equation (5). Alternatively the concept of weighting functions (Njoku and Kong, 1977) can be used to define an equivalent "sensing depth" which similarly defines the region of influence of the moisture and temperature profiles. While the entire soil moisture profile within the sensing depth will affect the emitted radiation, it is the sharp transitions in the profile that predominantly influence the emissivity. Most commonly the surface soil moisture and the near-surface moisture gradient are the dominant moisture profile parameters for soil emission. Thus, it is often found that variations in brightness temperature are related most closely to the moisture content in a shallow near-surface region within the sensing depth. This region is sometimes referred to separately as the "moisture sensing depth". As a practical rule of thumb, it is often stated that in the frequency range 1-3 GHz the moisture sensing depth corresponds approximately to the top 2-5 cm of soil (e.g. Schmugge et al., 1992), This is a useful approximation, but it is a simplification since the actual moisture sensing depth will depend on both the magnitude of the moisture content and the profile shape.

2,4 *Surface Roughness*

Rough surfaces (with uniform moisture profiles) may also be characterized by a surface emissivity (Equation (3)). The expressions for reflectivity (Equation (4) must be modified, however, for rough surfaces to take into account the effects of surface scattering. The reflectivities can be expressed as:

$$r_p(\theta, \phi) = \frac{1}{4\pi} \int \int_{2\pi} \left[\gamma_{pp}(\theta, \phi; \theta', \phi') + \gamma_{pq}(\theta, \phi; \theta', \phi')\right] d\Omega' \qquad (7)$$

in which the polarizations (p, q) refer to (h, v), *or* vice versa, and γ_{pp} and γ_{pq} are the co- and cross-polarized bistatic scattering coefficients for radiation scattered from an incident direction (8, ϕ) into a scattered direction (8', ϕ'). The solid angle integration is taken over the upper hemisphere. The bistatic coefficients are equal to the radar backscattering coefficients when (8, ϕ) = (8', ϕ'). In practice it is difficult to compute the emissivity using Equation (7) since this requires deriving expressions for the scattering coefficients and performing a two-dimensional integral. The scattering coefficients can be computed by assuming either a deterministic form or a statistical distribution for the surface roughness, such as periodic, as with a furrowed field, or randomly rough, as is more often the case in natural environments. Randomly rough surfaces may be represented statistically in terms

of two parameters: the height standard deviation, σ, and the horizontal correlation length, 1. Many approaches to deriving theoretical expressions for emissivity have been developed using these parameters (e.g. Fung and Eom, 1981; Tsang and Newton, 1982). Although they provide insight into the scattering mechanisms these expressions are not easy to use since they require detailed knowledge of the soil surface height and slope statistics, and their computational accuracy is often limited in practical situations.

A simpler, semi-empirical expression for rough surface reflectivity has been developed (Wang and Choudhury, 1981; Wang et al., 1983) which also includes two surface parameters: a height parameter, h' (which is related to the height standard deviation, σ), and a polarization mixing parameter, Q:

$$r_p = [Q\ r_{0q} + (1-Q)\ r_{0p}] \exp(-h') \qquad (8)$$

In this expression the reflectivities r_{0p} and r_{0q} are the reflectivities the medium would have if the surface were smooth. Thus, Equation (8) maybe considered as a modification of the smooth surface reflectivity (for which the parameters Q and h' are zero). The parameters Q and h' and their dependencies on frequency, height standard deviation, and viewing angle must be determined experimentally. Values for Q and h' have been determined for some soil roughness conditions from ground-based radiometer observations. However the experimental database is currently too limited to validate quantitatively these roughness pararneterizations over a substantial range of conditions. For analysis of data at 1.4 GHz, when surface roughness conditions may be unknown, a value of zero is often assigned to Q, and a value between O and 0.3 is typically assumed for h' (Jackson, 1993).

Figures 8(a) and (b) show experimentally the effects of surface roughness on brightness temperature as a function of moisture content and angle, respectively. In all cases surface roughness decreases the reflectivity (increases the brightness temperature) and decreases the difference between the vertically and horizontally polarized brightness temperatures. This is in agreement with the functional form of Equation (8). The sensitivity of brightness temperature to soil moisture decreases significantly as the surface roughness increases, thus corrections for roughness are necessary to obtain accurate soil moisture estimates. Within certain broad classes of surface types the natural variability of roughness can be small enough to be corrected using simple estimates of the roughness parameters.

2.5 Vegetation

Vegetation absorbs, emits, and scatters microwave radiation. The vegetation can be modeled for simplicity as a single homogeneous layer above the soil. At low frequencies the effects of scattering at the surface and within the volume of the vegetation are small and are often neglected, The brightness temperature 'of a two layer soil-vegetation medium can then be written as:

$$T_{B_p} = e_p T_e \exp(-\tau) + T_c (1 - \exp(-\tau)) (1 + r_p \exp(-\tau)) \quad (9)$$

where T_c is the vegetation temperature, T_e is the soil effective temperature, τ is the vegetation opacity, and e_p and r_p are the emissivity and reflectivity of the underlying soil surface. This expression is obtained by considering the different paths for radiative transfer through the medium. A key parameter is the vegetation optical thickness, τ. For small values oft (low vegetation) Equation (9) reduces to $T_{Bp} = e_p T_e$, i.e. the observed brightness is approximately equal to the soil brightness temperature, while for large τ (thick vegetation) the observed brightness temperature approaches $T_{Bp} = T_c$, i.e the brightness temperature approaches the temperature of the vegetation canopy which appears like a blackbody of unit emissivity. In this case the soil is completely masked by the vegetation.

The value oft depends on the vegetation type (geometrical structure of leafy and woody components), the water content of the vegetation, and the wavelength. A simple theoretical expression for the vegetation opacity, derived from an expression given originally by Kirdiashev et al. (1979) is:

$$\tau = A \nu \quad W \varepsilon_c'' / \cos \quad \theta \quad (lo)$$

where A is a structure parameter related to the geometry of the vegetation, v is the frequency, W is the total water content of the vegetation in kg/m^2, and ε_c'' is the imaginary part of the dielectric constant of the water in the vegetation. Typical values of W range from less than 0.5 kg/m^2 for light grass to 10 kg/m^2 and greater for forests. Figure 9 shows the computed dependence of emissivity on soil moisture using this expression for soil covered by varying amounts of vegetation, using parameters for τ derived from experimental measurements at 1.4 GHz (Schmugge, 1990). It is evident that increasing amounts of vegetation decrease the sensitivity to soil moisture. Thus, soil moisture

estimates require correction for the effects of vegetation and become increasingly unreliable as the opacity of the vegetation layer increases.

3.0 RETRIEVAL OF SOIL MOISTURE

The previous section has outlined the main factors affecting soil microwave emission which, in addition to the soil moisture, include the soil texture, surface roughness, soil and vegetation temperature, and vegetation type and 'water content. To retrieve soil moisture from brightness temperature observations corrections must be made for these additional factors. The magnitudes of the corrections can be reduced significantly 'by using low-frequency observations in the 1-3 GHz range. In order to discuss specific retrieval methods for soil moisture reference must first be made to the frequency and scanning configuration of the observational system.

3.1 *Observing System Considerations*

In developing spaceborne system concepts for a soil moisture radiometer, previous studies have focussed mainly on a single frequency system operating at 1.4 GHz with horizontal polarization, and providing 10 km spatial resolution with a global mapping capability every three days. This is the basis, for example, of the Electronically Scanned Thinned Array Radiometer (ESTAR) concept (NASA, 1987; LeVine et al., 1989; Swift, 1993). This concept is illustrated in Figure 10. The spaceborne system would operate at art altitude of about 350 km and provide a cross-track-scanning swath width of ±40° (1200 km). The possibility of additional frequencies at 2.7 and 5 GHz and an option for a fixed viewing-angle conical scan, with dual horizontal and vertical polarizations have also been considered, The discussion on retrievals will focus initially on an assumed 1,4 GHz horizontally-polarized system, and will then discuss briefly retrievals using other observational configuration options.

3.2 *Single-Frequency, Single-Polarization Retrieval*

If only a single measurement channel is available, information from other sources is needed to make corrections for vegetation, roughness, temperature, and texture. A basic approach when analyzing data from single-channel aircraft and ground-based

measurements is to make corrections sequentially for each of the above effects (e.g. Wang, 1989; Jackson, 1993). A land cover database or other a priori information can be used to determine a broad classification of surface type within the measurement footprint, e.g forest, grassland, broadleaf crops, etc. An estimate of the vegetation opacity, τ, can be obtained from an independent measurement such as an optical/infrared remotely sensed vegetation index,. A surface temperature estimate can be obtained either from a near-simultaneous thermal infrared remotely sensed measurement or by extrapolation from a local surface air temperature measurement, Equations (3) and (9) can then be used to obtain an estimate of the soil rough surface emissivity, assuming that the soil effective temperature and canopy temperature are approximately equal. This is only feasible if the opacity τ is sufficiently small that Equation (9) can be inverted without unacceptable error amplification. Knowledge of soil texture and roughness, obtained from a-priori soil data and land management practice information, can then be used to determine the appropriate soil moisture versus emissivity curve to use in estimating the soil moisture.

Variations on the above procedure have been used successfully to estimate soil moisture as demonstrated under some well-controlled and -instrumented conditions. Figure 11 shows results of soil moisture estimates derived from 1.4 GHz aircraft radiometer measurements as part of the FIFE experiment (Wang et al., 1989). Similar results were obtained in the MONSOON 90 experiment (Schmugge et al., 1992). Results from more recent aircraft experiments in the Little Washita Watershed in 1992 are described by Jackson (1994). For operational applications over larger and more heterogeneous areas, the retrieval approach described above contains some pitfalls for a spaceborne system, especially in the reliance on ancillary data which may itself be unreliable. Another difficulty is the necessity for inserting an angular dependence into the corrections, since in a cross-track scanning mode each footprint views the surface at a different viewing angle.

3.2 *Multichannel Conical-scanning Methods*

Multi-frequency, multi-polarization radiometers with conical scanning have operated in space for many years. These systems, such as the Scanning Multichannel Microwave Radiometer (SMMR) and the Special Sensor Microwave/Imager (SSM/I), operate at higher microwave frequencies than are suitable for soil moisture sensing (6.6 - 90 GHz) but have two significant operational advantages. The first is that by providing several independent channels of data, each with a different sensitivity to the surface geophysical variables, it is possible to make simultaneous retrievals of the surface

parameters provided the number of measurement channels exceeds the number of parameters to be estimated, In this approach, higher frequency and orthogonally-polarized channels can be used to make corrections for the effects of surface roughness and vegetation on the soil moisture estimates. Initial steps in this direction have been undertaken in the analysis of SMMR data over land (Kerr and Njoku, 1990). "Another advantage of these systems is that by using conical-scanning antennas the instruments view the surface at the same angle at all positions in the swath. Hence no corrections for angular effects are necessary. A multichannel conical-scanning configuration may add considerable complexity to a low frequency system such as ESTAR, but its advantages merit continued consideration.

3.3 Retrieval of Soil Profile Information

Since the sensing depth in moist soils varies with wavelength it is possible, in principle, to use multifrequency measurements to estimate the moisture contents at different depths in the soil, i.e. to derive information on the moisture profile within the sensing depth of the longest wavelength used, This technique was suggested by Njoku and Kong (1977) to obtain a surface value and slope of the soil moisture profile; more recently Reutov and Shutko (1990) have also investigated this approach. However, the sensing depth places a limit on the ability of remote sensing instruments to retrieve soil moisture at depths much greater than several centimeters.

A more productive method for estimating the soil moisture profile has been described by Entekhabi et al. (1994), This approach uses a coupled soil moisture and heat flux model, and remotely sensed measurements of surface moisture and temperature, in a Kalman filtering assimilation procedure which effectively extrapolates the remotely sensed surface information to lower depths in the soil. Results of a simulation test of this approach are shown in Figures 12 and 13. Figure 12 shows a set of simulated soil moisture and temperature profiles generated using the model of Milly and Eagleson (1980) representing drying conditions over a one-week period, A corresponding set of hourly brightness temperatures (to simulate microwave observations) and surface temperatures (to simulate infrared observations) are computed from the model-generated profiles. The retrieval scheme is given an initial guess for the moisture and temperature profiles (in this case an intentional y poor guess is given for the moisture profile - Figure 13a). In the retrieval scheme, the model system equation is used to forecast and propagate the state variables (moisture and temperature profiles). At each hour the state is updated using the

microwave and surface temperature observations. In Figure 13b the true moisture profile (open circles) is shown for each half-day. Also shown-is the estimated profile generated by the Kalman filter (dark circles) as well as the "open-loop" profile (for which no constraining observations are used and the system is simply propagated from the initial guess). The filter estimates converge to the true profile after about four days. The open-loop profile, without the information provided by the remotely sensed observations, dries out rapidly and does not converge to the true profile. These results indicate the advantages to be gained in developing retrieval methods that combine physical models of the dynamic soil state and physically based remote sensing models in an optimal assimilation scheme. The effects of geophysical and remote sensing "noise" in the system can also be systematically analyzed to provide estimates of the stability and accuracy of the retrievals,

4.0 CONCLUSION

A review has been provided of the physical basis for remote sensing of soil moisture using microwave radiometry. " The current state of the art indicates that surface soil moisture measurements from space are feasible in regions of bare soil or low vegetation cover using a system with frequencies in the range 1-5 GHz. Such measurements, acquired on a global and repetitive basis, would be extremely useful for hydrologic and climate studies. The perturbing effects of soil texture, surface roughness, and vegetation cover are well understood qualitatively, but soil moisture retrieval techniques have been validated mostly on a local basis and would benefit from further testing for regional and global applications, The effect on soil moisture retrievals of the spatial heterogeneity of soil properties within a radiometer footprint also needs further study. The feasibility of moisture profile information retrieval for bare soils has also been demonstrated using model and data simulations, however experimental validation and extension of this technique to natural terrain require further research,

5.0 ACKNOWLEDGMENT

This work was performed in part at the Jet Propulsion Laboratory, California Institute of Technology, under contract to the National Aeronautics and Space Administration. Dr. Entekhabi's research was supported by NASA Grant NAGW 2942.

6.0 REFERENCES

Choudhury, B. J., T. J. Schmugge, and T. Mo (1982): A parameterization of effective soil temperature for microwave emission. J. Geophys. Res., 87, 1301-1304.

Dobson, M. C., F. T. Ulaby, M. T. Hallikainen, and M. El-Reyes (1985): Microwave dielectric behavior of wet soil - Part II: Dielectric mixing models, IEEE Trans. Geosci. Rem. Sens., GE-23, 35-46.

Entekhabi, D., H. Nakamura, and E. G. Njoku (1993): Solving the inverse problem for soil moisture and temperature profiles by the sequential assimilation of multifrequency observations. IEEE Trans. Geosci. Rem, Sens. (in press),

Fung, A. K, and H, J. Eom (1981): Emission from a Rayleigh layer with irregular boundaries. J. Quant. Spectr. Radiat. Transfer, 26,397-409.

Hoekstra, P. and A, Delaney (1974): Dielectric properties of soils at UHF and microwave frequencies. J. Geophys. Res., 76,4922-4931.

Jackson, T. J. and P. E. O'Neill (1987): Salinity effects on the microwave emission of soil. IEEE Trans. Geosci. Rem. Sens., GE-25, 214-220.

Jackson, T. J. (1993): Measuring surface soil moisture using passive microwave remote sensing. Hydrological Processes, 7, 139-152.

Jackson, T. J. (1994): (This issue).

Kerr, Y. and E. G. Njoku (1990): A semiempirical model for interpreting microwave emission from semiarid land surfaces as seen from space. IEEE Trans. Geosci. Rem. Sens., 28,384-393.

Kirdiashev, K. P., A. A. Chukhlantsev, and A. M. Shutko (1979): Microwave radiation of the Earth's surface in the presence of vegetation. Radio Engin. Electron. 24,256-264.

Levine, D. M., T. T. Wilheit, R. Murphy, and C. T. Swift (1989): A multifrequency microwave radiometer of the future. IEEE Trans. Geosci. Rem. Sens., 27, 193-199.

Mill y, P. C. D. and P. S. Eagleson (1980): A" coupled transport of water and heat in a vertical soil column under atmospheric excitation. Report #258, Ralph M. Parsons Lab., Dept. of Civil Engineering, Massachusetts Institute of Technology, Cambridge; MA.

NASA (1987): HMMR Instrument Panel Report, Earth Observing System, Vol He. National Aeronautics and Space Administration, Washington, DC.

Njoku, E. G. and J. A. Kong (1977): Theory for passive microwave remote sensing of near-surface soil moisture. J. Geophys. Res., 82,3108-3118.

Reutov, E. A. and A. M. Shutko (1990): Microwave spectroradiometryof water content of nonuniformly moistened soil with a surface transition layer. Sov. J. Remote Sensing, 6, 72-79.

Schmugge, T. J. (1990): Measurements of surface soil moisture and temperature, in: Remote Sensing of Biosphere Functioning (R. J. Hobbs and H. A, Mooney$, Eds.), Springer-Verlag, New York.

Schmugge, T. J., T. J. Jackson, W. P. Kustas, and J. R. Wang (1992): Passive microwave remote sensing of soil moisture: results from HAPEX, FIFE and MONSOON 90. ISPRS J. Photogramm. Rem. Sens., 47, 127-143.

Swift, C. T. (1993): ESTAR - The electronically scanned thinned array radiometer for remote sensing measurement of soil moisture and ocean salinity. NASA Technical Memorandum #4523, NASA/Goddard Space Flight Center, Greenbelt, MD.

Tsang, L., E. Njoku, and J, A. Kong (1975): Microwave thermal emission from a stratified medium with nonuniform temperature distribution. J. Appl. Phys., 46, 5127-5133.

Tsang, L. and R. W. Newton (1982): Microwave emission from soils with rough surfaces, J. Geophys. Res., 87, 9017-9024.

Ulaby, F. T., R. K, Moore, and A. K. Fung (1986): Microwave Remote Sensing, Active and Passive, Volume III: From Theory to Applications, Artech House, Dedham, MA.

Wang, J. R, and T. J. Schmugge (1980): An empirical model for the complex dielectric permittivity of soils as a function of water content, IEEE Trans. Geosci. Rem. Sens., GE-18,288-295.

Wang, J. R. and B. J. Choudhury (1981): Remote sensing of soil moisture content over bare field at 1.4 GHz frequency. J. Geophys. Res., 86,5277-5282.

Wang, J. R., P. E. O'Neill, T. J. Jackson, and E. T. Engman (1983): Multifrequency measurements of the effects of soil moisture, soil texture, and surface roughness. IEEE Trans. Geosci. Rem. Sens., GE-21, 44-51.

Wang, J. R., T. J. Schmugge, J. C. Shiue, and E. T. Engman (1989): Mapping surface soil moisture with L-band radiometric measurements. Remote Sensing of Environment, 27,305-312.

FIGURE CAPTIONS

Figure 1: Configuration for a radiometer viewing the Earth surface from a remote platform.

Figure 2: Dielectric constant as a function of volumetric soil moisture for five soils at 1.4 GHz. The curves have been drawn through measured data points. (From Ulaby et al., 1986).

Figure 3: Dielectric constant of sand as a function of frequency and moisture (Njoku and Kong, 1977).

Figure 4: Microwave soil penetration depth as a function of frequency and moisture content.

Figure 5: Computed and observed relationships between emissivity and soil moisture for bare, smooth fields (loamy sand) at 1.4 GHz. (From Jackson and O'Neil (1987).

Figure 6: Computed emissivity as a function of viewing angle for a sandy soil with moisture contents of 5% and 30%. The curves are for frequencies of 0.675 and 14 GHz, and indicate the different behavior of the vertical and horizontal polarizations.

Figure 7: Representative profiles of (a) moisture and (b) temperature for Phoenix, Arizona soil. Curves are labeled by number of days after irrigation. (c) ScatterPlots of effective temperature versus surface temperature computed for. profiles in (a) and (b). (From Choudhury et al., 1982)

Figure 8: Variations in brightness temperature as a function of (a) moisture content (b) angle for soils, of different roughness at 1.4, 5, and 10.7 GHz. (From Wang et al., 1983).

Figure 9: Effects of vegetation on the relationship between emissivity and soil moisture, computed for values of water content, W, typical of some vegetation types. (From Schmugge, 1990).

Figure 10: The spaceborne ESTAR concept. The long stick antennas are aligned in the direction of motion to give real aperture resolution along the satellite ground track. Resolution across track is obtained synthetically through signal processing. (From NASA, 1987).

Figure 11: Contours of soil moisture in the top 5 cm layer derived from aircraft radiometric measurements at 1.4 GHz: (a) 28, May 1987; (b) 4 June 1987. (From Wang et al., 1989).

Figure 12: (a) Twice daily profiles of soil matric head under conditions of 5 mm/day evaporation and initially ψ = -50 cm uniform conditions, (b) Same as (a), but for the soil temperature profile, with initially T =20 *C uniform conditions and periodic (diurnal) radiative forcing. (From Entekhabi et al., 1994).

Figure 13: (a) The initial soil matric head for the true profile (open circles) at ψ = -50 cm. The initial guess for the retrieval algorithm is intentionally set at the poor estimate of-300 cm (dark symbols). (b) The soil matric head profiles every half day for the true situation (open circles), retrieval algorithm (dark circles), and "open-loop" simulation (open triangles). (From Entekhabi et al., 1994).

Figure 1

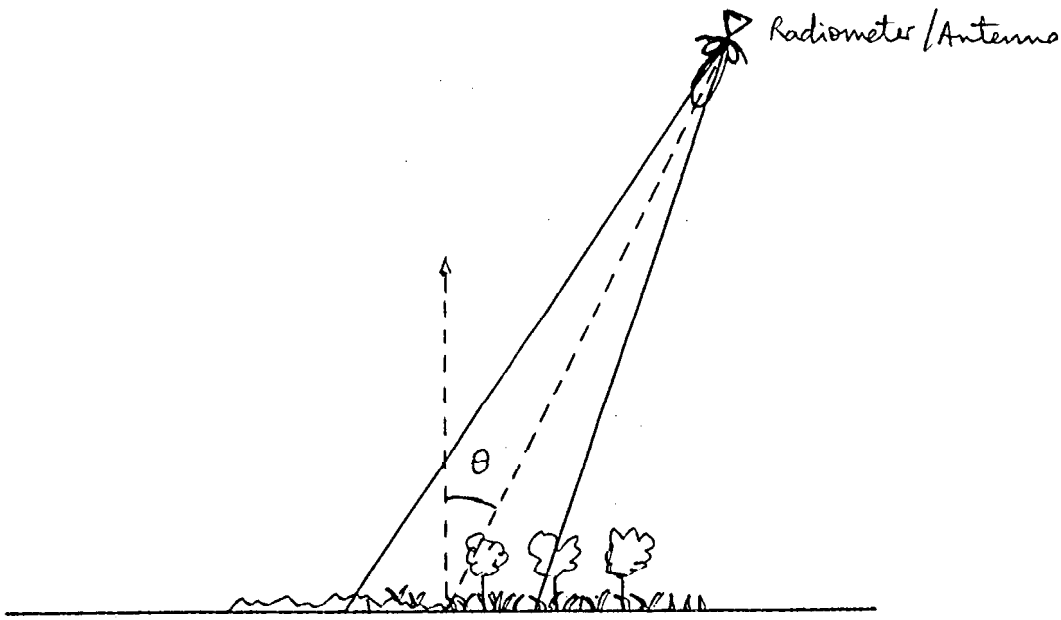

Figure 2

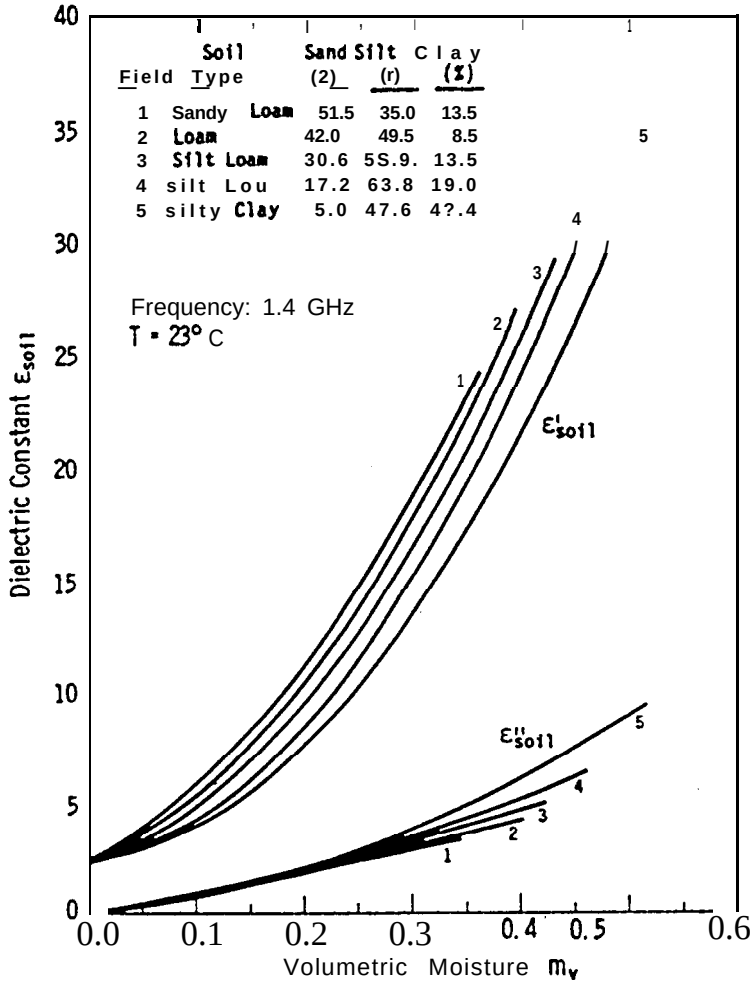
Soil
Field Type
Sand (2)
Silt (r)
Clay (%)
1 Sandy Loam 51.5 35.0 13.5
2 Loam 42.0 49.5 8.5
3 Silt Loam 30.6 5S.9. 13.5
4 silt Lou 17.2 63.8 19.0
5 silty Clay 5.0 47.6 4?.4
Frequency: 1.4 GHz
T = 23° C
Dielectric Constant ϵ_{soil}
ϵ'_{soil}
ϵ''_{soil}
Volumetric Moisture m_v
0
5
10
15
20
25
30
35
40
0.0
0.1
0.2
0.3
0.4
0.5
0.6

Figure 3

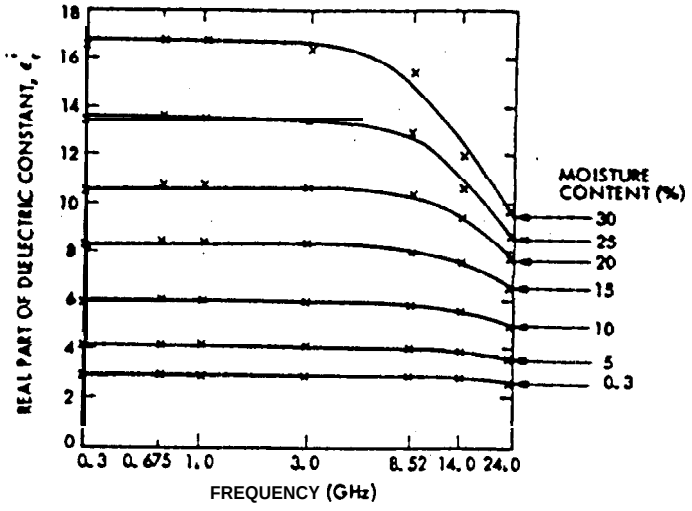
REAL PART OF DIELECTRIC CONSTANT, ϵ'_r
18
16
14
12
10
8
6
4
2
0
0.3
0.675
1.0
3.0
8.52
14.0
24.0
FREQUENCY (GHz)
MOISTURE CONTENT (%)
30
25
20
15
10
5
0.3

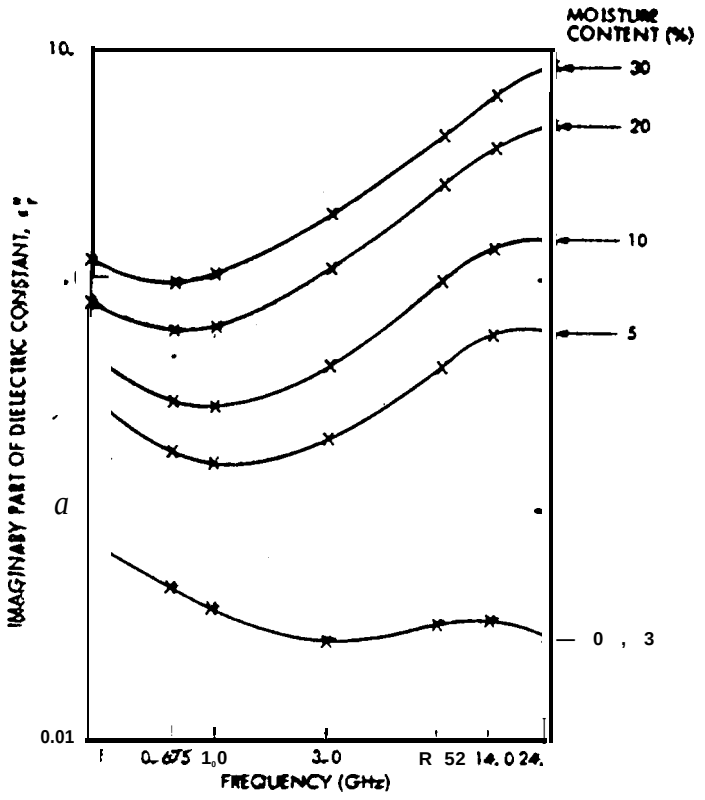
IMAGINARY PART OF DIELECTRIC CONSTANT, ϵ''_r
10.
1
0.01
0.675
1.0
3.0
R 52
14.0
24.
FREQUENCY (GHz)
MOISTURE CONTENT (%)
30
20
10
5
0 , 3

Figure 4

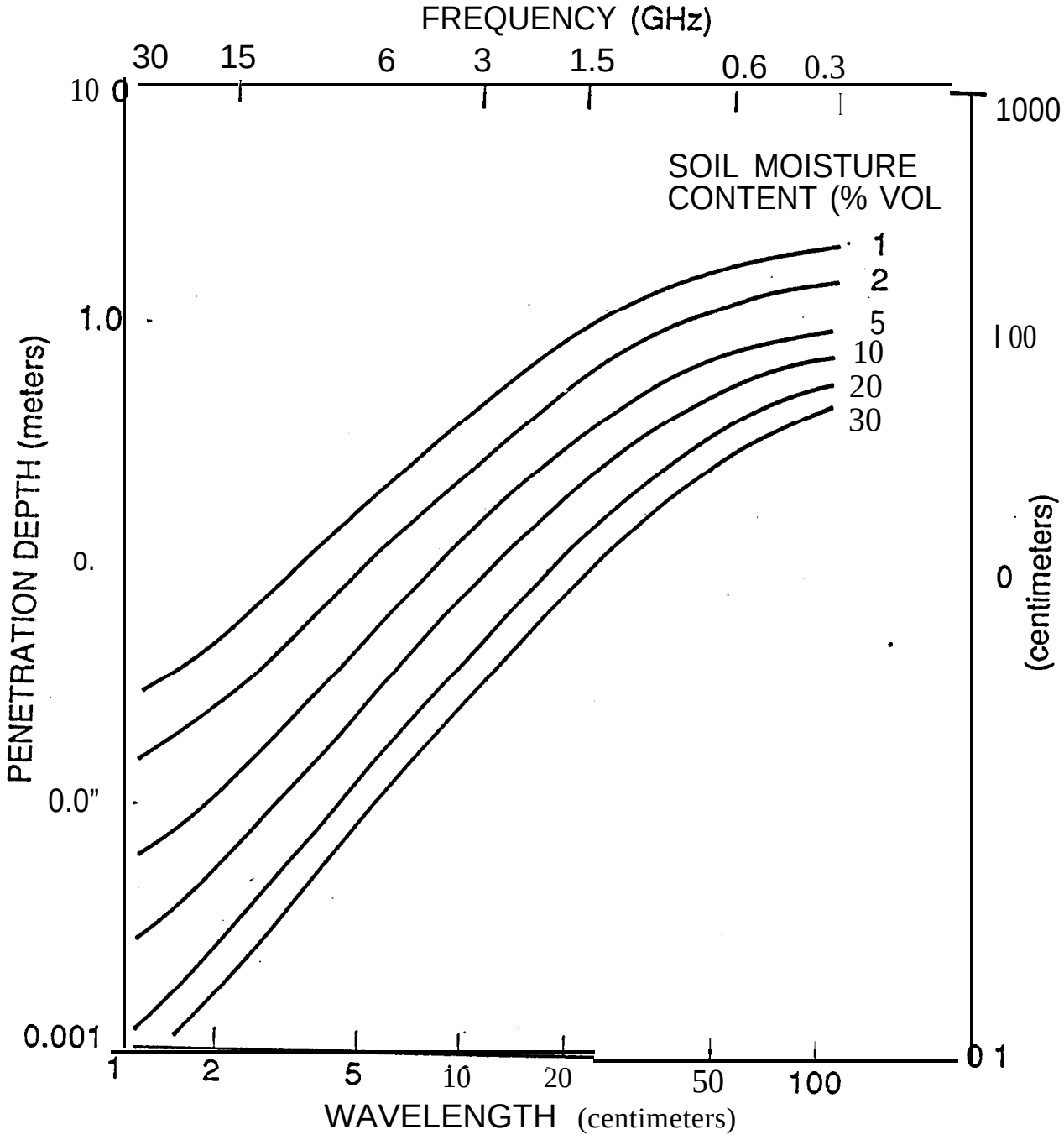
FREQUENCY (GHz)
30
15
6
3
1.5
0.6
0.3
10 0
1000
SOIL MOISTURE
CONTENT (% VOL
1
2
5
10
20
30
1.0
I 00
PENETRATION DEPTH (meters)
0.
0
(centimeters)
0.0"
0.001
0 1
1
2
5
10
20
50
100
WAVELENGTH (centimeters)

Figure 5

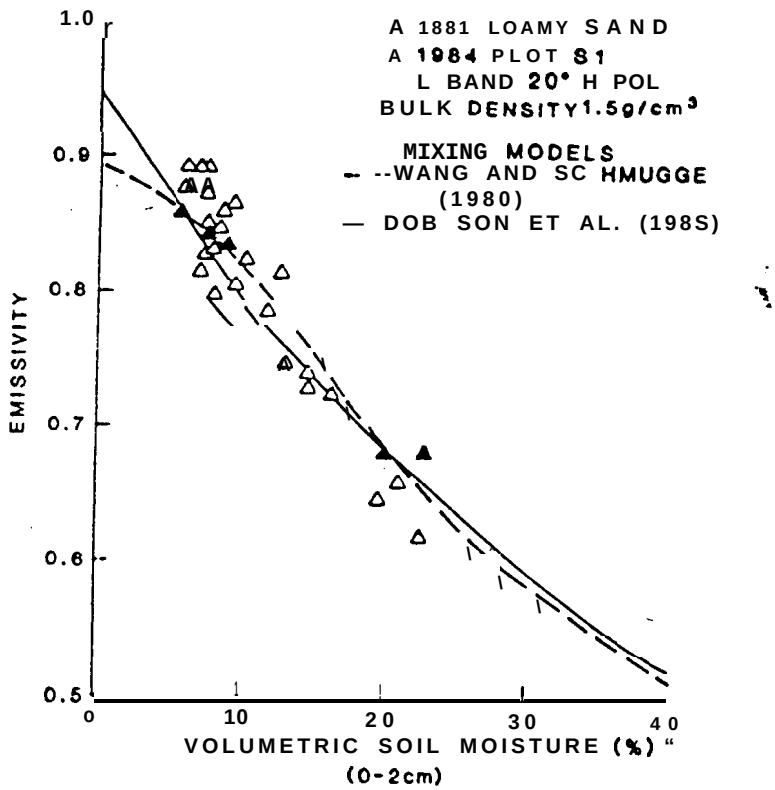
A 1881 LOAMY SAND
A 1984 PLOT S1
L BAND 20° H POL
BULK DENSITY 1.5g/cm³
MIXING MODELS
--WANG AND SC HMUGGE (1980)
— DOB SON ET AL. (198S)
EMISSIVITY
1.0
0.9
0.8
0.7
0.6
0.5
0
10
20
30
40
VOLUMETRIC SOIL MOISTURE (%)
(0-2cm)

Figure 6

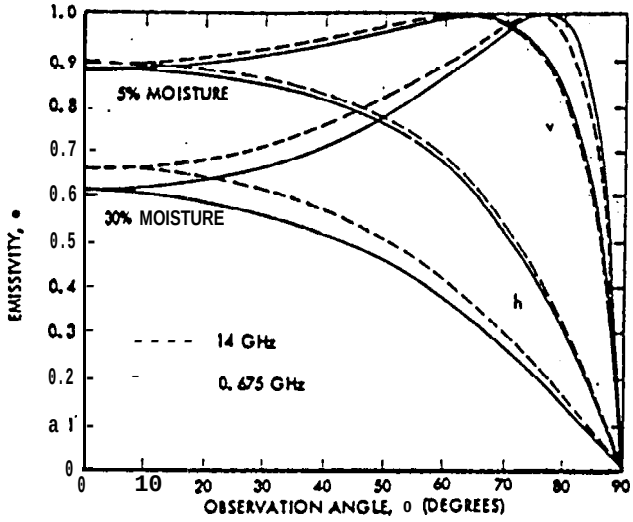
1.0
0.9
0.8
0.7
0.6
0.5
0.4
0.3
0.2
0.1
0
EMISSIVITY, e
5% MOISTURE
30% MOISTURE
v
h
14 GHz
0.675 GHz
0
10
20
30
40
50
60
70
80
90
OBSERVATION ANGLE, θ (DEGREES)

Figure 7

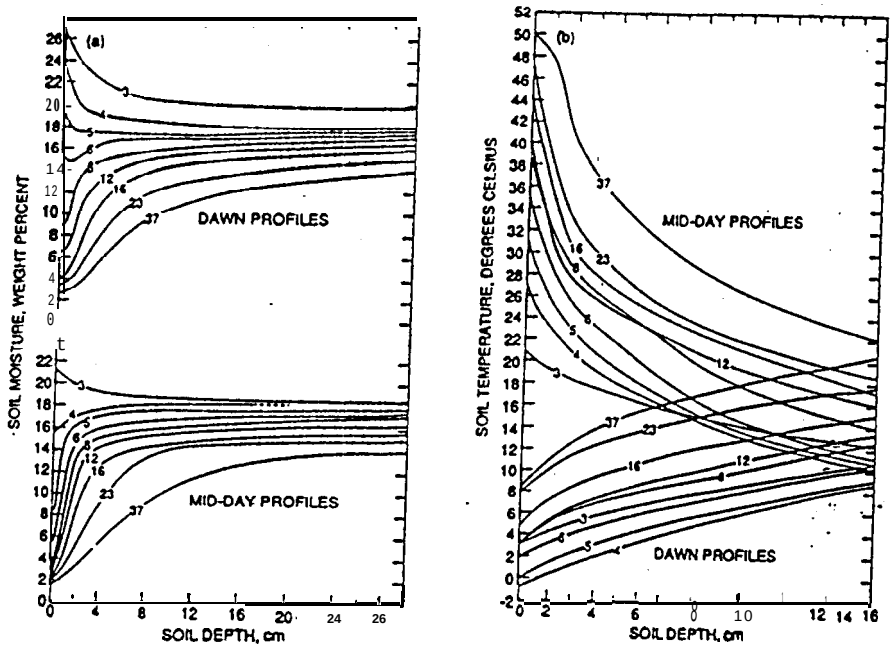
(a)
SOIL MOISTURE, WEIGHT PERCENT
DAWN PROFILES
MID-DAY PROFILES
SOIL DEPTH, cm
(b)
SOIL TEMPERATURE, DEGREES CELSIUS
MID-DAY PROFILES
DAWN PROFILES
SOIL DEPTH, cm

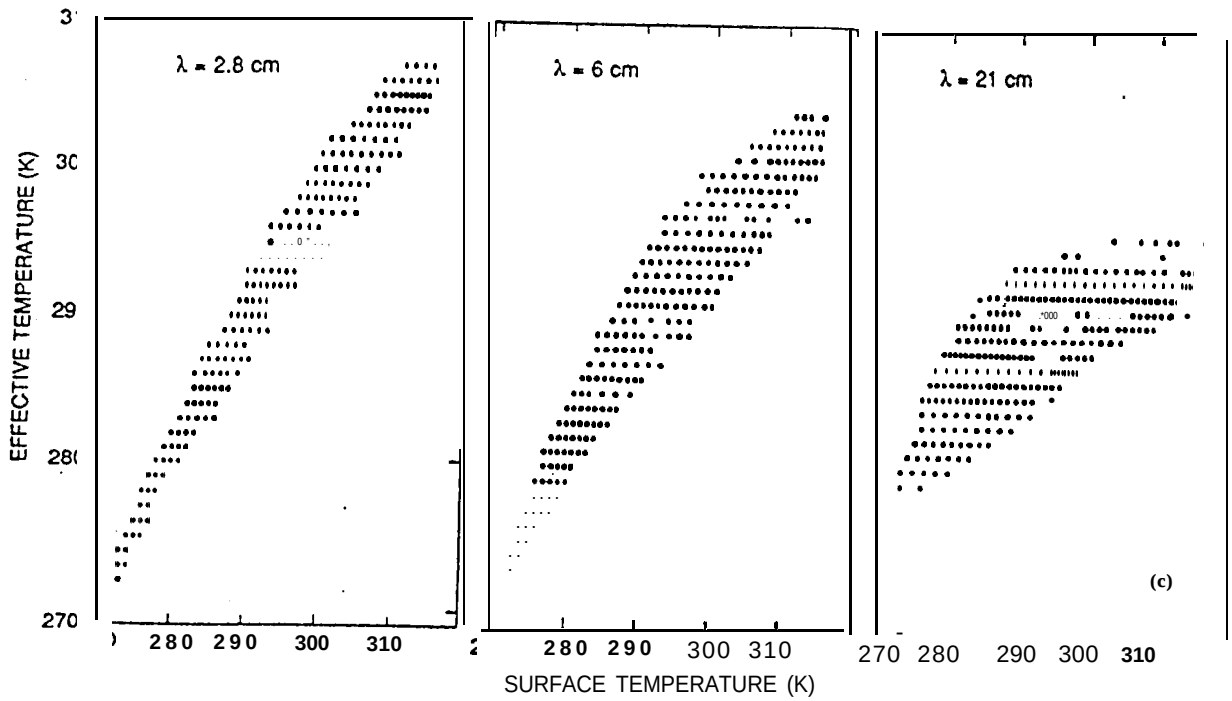
λ = 2.8 cm
λ = 6 cm
λ = 21 cm
EFFECTIVE TEMPERATURE (K)
SURFACE TEMPERATURE (K)
(c)

Figure 8

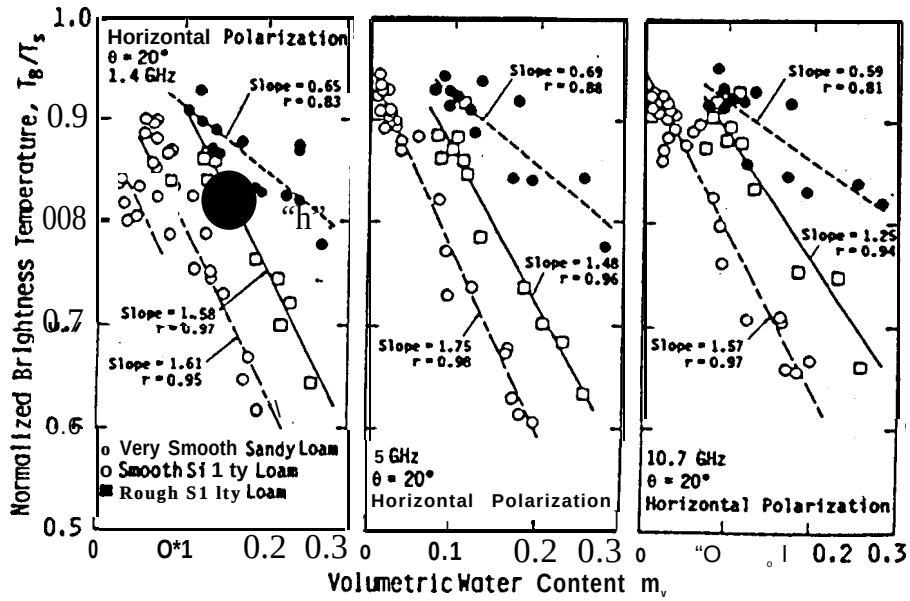
Horizontal Polarization
θ = 20°
1.4 GHz
Slope = 0.65
r = 0.83
Slope = 1.58
r = 0.97
Slope = 1.61
r = 0.95
o Very Smooth Sandy Loam
o Smooth Silty Loam
■ Rough Silty Loam
Slope = 0.69
r = 0.88
Slope = 1.48
r = 0.96
Slope = 1.75
r = 0.98
5 GHz
θ = 20°
Horizontal Polarization
Slope = 0.59
r = 0.81
Slope = 1.25
r = 0.94
Slope = 1.57
r = 0.97
10.7 GHz
θ = 20°
Horizontal Polarization
Normalized Brightness Temperature, T_B/T_s
Volumetric Water Content m_v

(a)

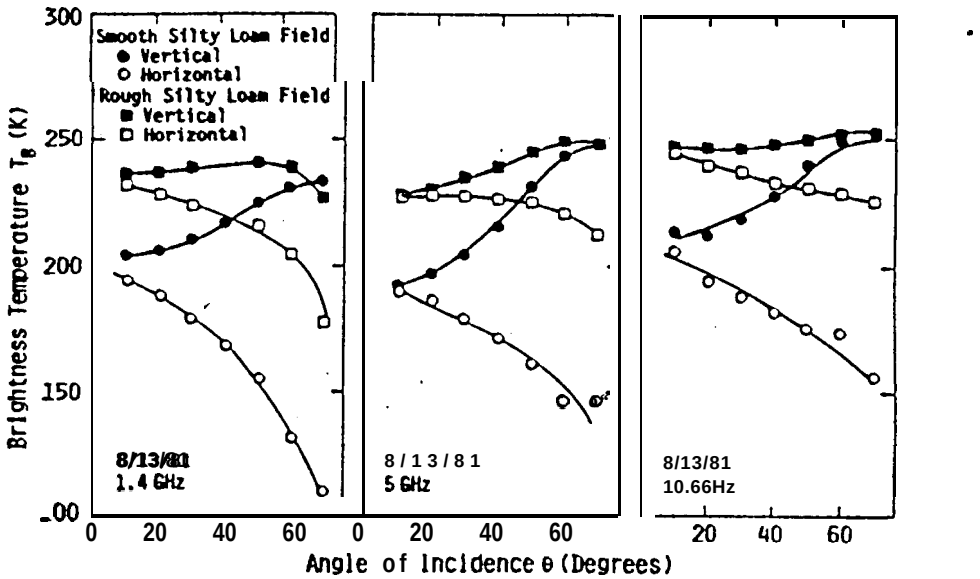
Smooth Silty Loam Field
● Vertical
○ Horizontal
Rough Silty Loam Field
■ Vertical
□ Horizontal
8/13/81
1.4 GHz
8/13/81
5 GHz
8/13/81
10.66Hz
Brightness Temperature T_B (K)
Angle of Incidence θ (Degrees)

(b)

Figure 9

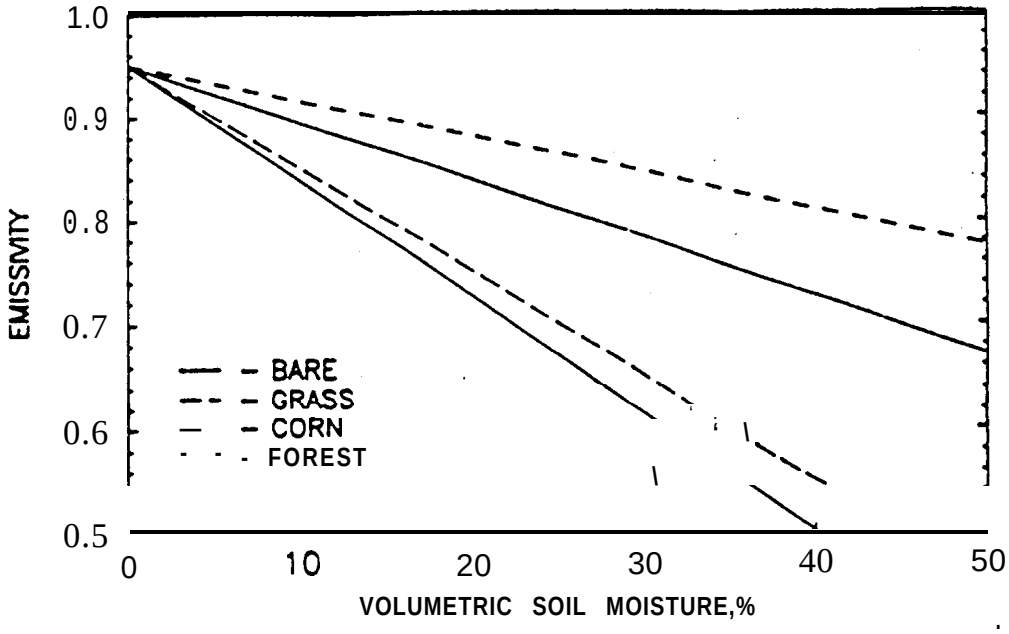
1.0
0.9
0.8
0.7
0.6
0.5
EMISSIVITY
BARE
GRASS
CORN
FOREST
0
10
20
30
40
50
VOLUMETRIC SOIL MOISTURE,%

Figure 10

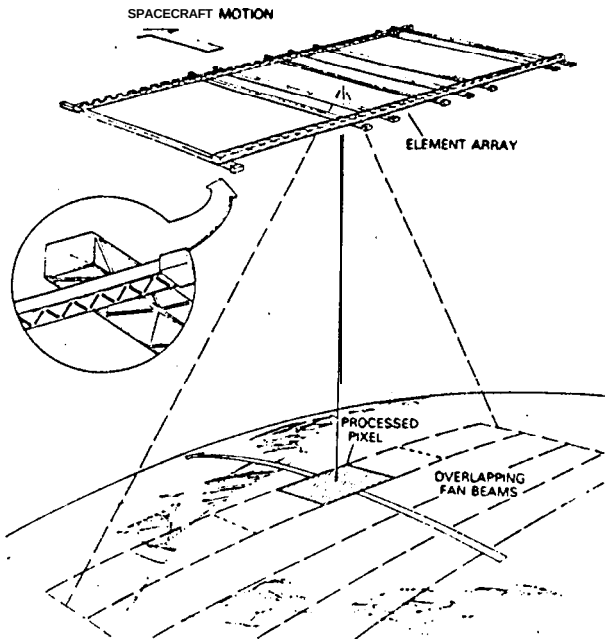
SPACECRAFT MOTION
ELEMENT ARRAY
PROCESSED PIXEL
OVERLAPPING FAN BEAMS

Figure 11

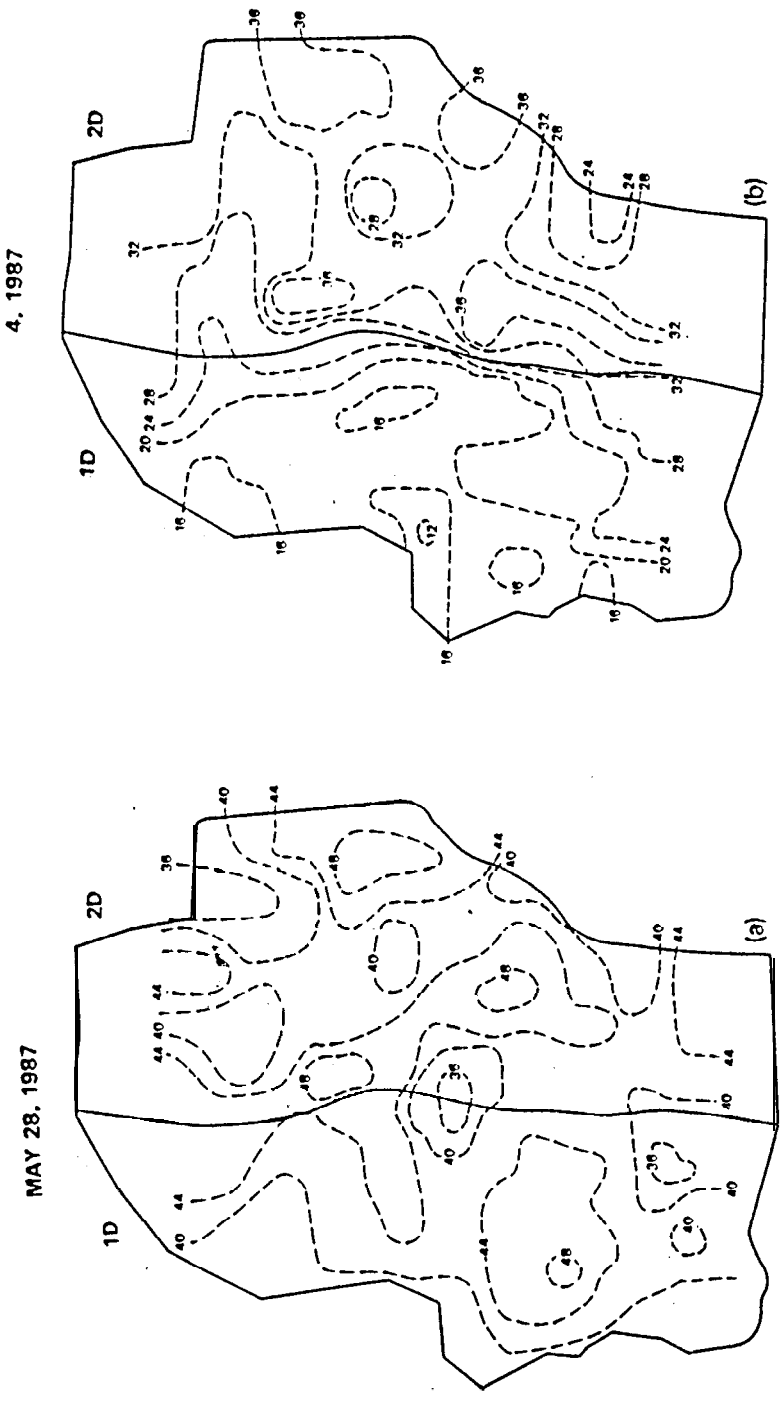

Figure 12

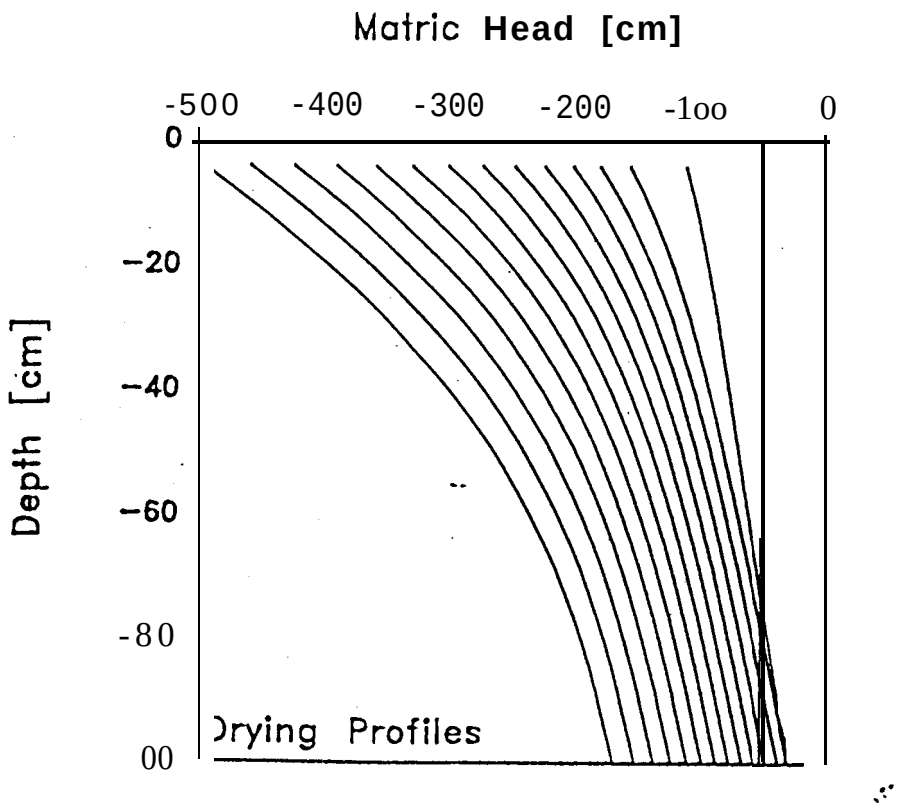
Matric Head [cm]
-500
-400
-300
-200
-1oo
0
0
-20
-40
-60
-80
00
Depth [cm]
Drying Profiles

(a)

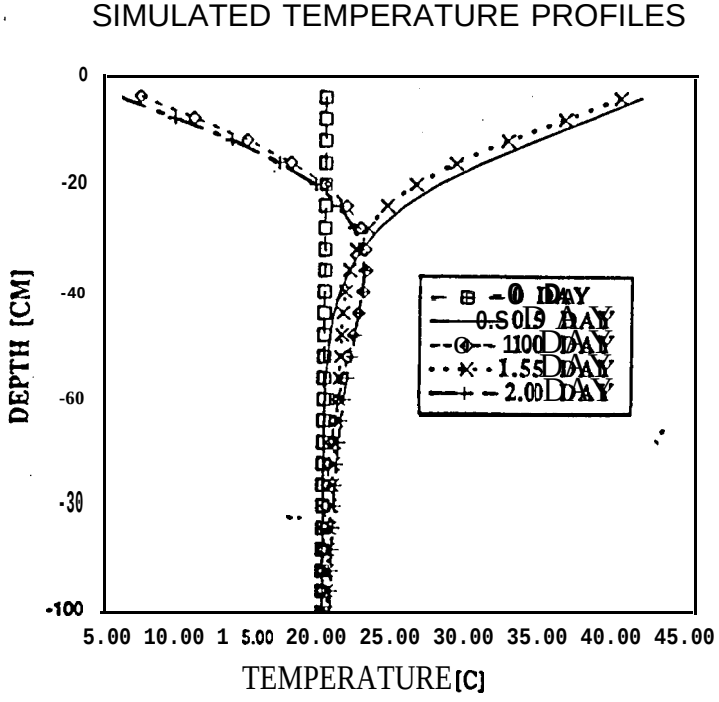
SIMULATED TEMPERATURE PROFILES
0
-20
-40
-60
-30
-100
DEPTH [CM]
0 DAY
0.50 DAY
1.00 DAY
1.55 DAY
2.00 DAY
5.00 10.00 15.00 20.00 25.00 30.00 35.00 40.00 45.00
TEMPERATURE [C]

(b)

Figure 13(a)

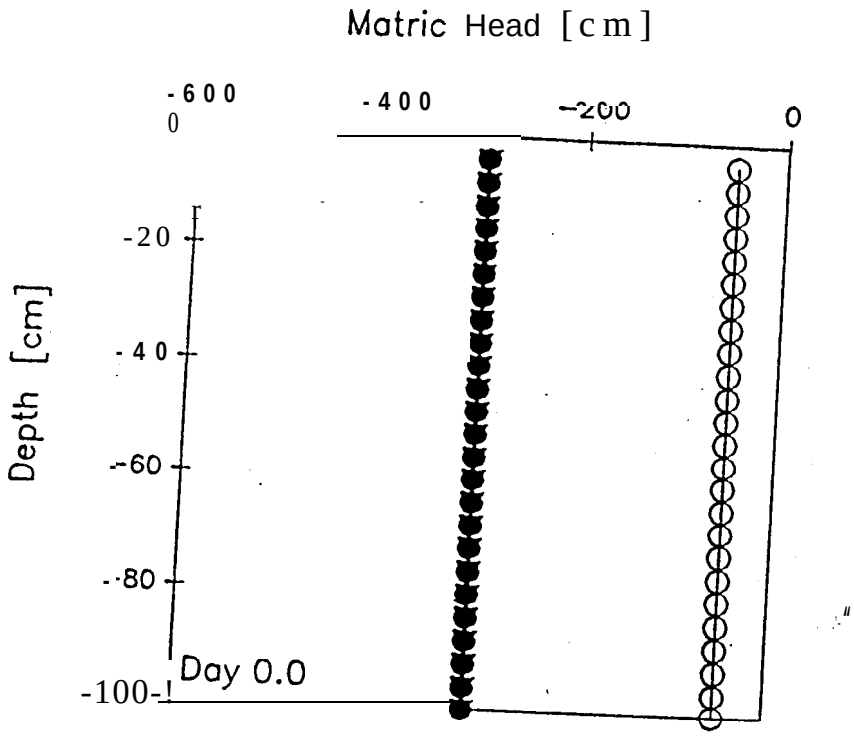

Figure 13(b)

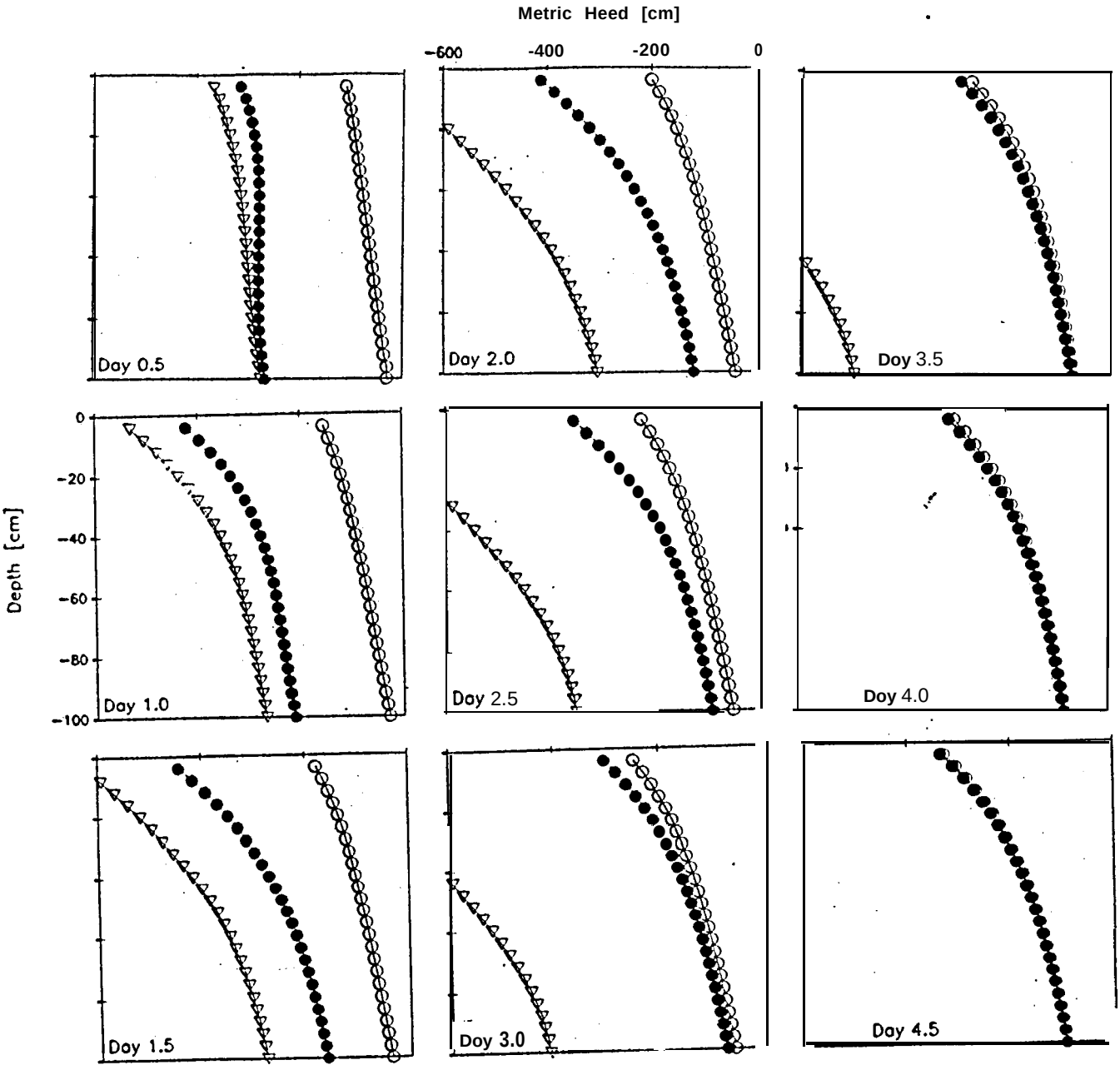
Metric Heed [cm]
-600
-400
-200
0
Depth [cm]
0
-20
-40
-60
-80
-100
Day 0.5
Day 2.0
Doy 3.5
Day 1.0
Day 2.5
Doy 4.0
Day 1.5
Day 3.0
Day 4.5